

# Molecular Dynamics Simulations of a Set of Isoniazid Derivatives Bound to InhA, the enoyl-*acp* Reductase From *M. tuberculosis*

KERLY F. M. PASQUALOTO,<sup>1</sup> MÁRCIA M. C. FERREIRA,<sup>1</sup>  
OSVALDO A. SANTOS-FILHO,<sup>2</sup> ANTON J. HOPFINGER<sup>2</sup>

<sup>1</sup>Department of Physical Chemistry, Laboratory for Theoretical and Applied Chemometrics, Institute of Chemistry, Building H, Room 219, State University of Campinas, UNICAMP, Campinas, SP 13084-971, POB 6154, Brazil

<sup>2</sup>Laboratory of Molecular Modeling and Design (M/C-781), College of Pharmacy, University of Illinois at Chicago, 833 South Wood Street, Chicago, Illinois 60612-7231, USA

Received 27 December 2005; accepted 15 March 2006

Published online 22 June 2006 in Wiley InterScience (www.interscience.wiley.com).

DOI 10.1002/qua.21055

**ABSTRACT:** Ligand-receptor molecular dynamics simulations (MDS) were carried out for a set of hydrazides bound to the enoyl-*acp* reductase from *M. tuberculosis*, InhA (PDB entry code 1zid). The hypothesized active conformations resulting from a previous receptor-independent (RI) 4D-QSAR analysis and related optimum model/alignment were used in this study. The molecular dynamics simulations (MDS) protocol employed 500000 steps for each ligand-receptor complex, the step size was 0.001 ps (1 fs), and the simulation temperature was 310 K, the same temperature used in the biological assay. An output trajectory file was saved every 20 simulation steps, resulting in 25,000 conformations. The hydration shell model was used to calculate the solvation energy of the lowest-energy conformation obtained from each MDS. Structural parameters as well as binding energy contributions were considered in this analysis. The thermodynamic descriptors  $EL_{E1,4}$ ,  $EL_{tors}$ ,  $EL_{vdW}$ ,  $EL_{el}$ , and  $EL_{el+Hb}$  appear to be more relevant to the biological activity. These findings can be meaningful for developing QSAR studies and for designing new antituberculosis agents. © 2006 Wiley Periodicals, Inc. *Int J Quantum Chem* 106: 2689–2699, 2006

**Key words:** hydrazides; enoyl-*acp* reductase; molecular dynamics simulations; structure-based design; tuberculosis

Correspondence to: K. F. M. Pasqualoto; e-mail: kerly@netpoint.com.br

Contract grant sponsors: CNPq; FAPESP.

## Introduction

**E**nzymes that form the biosynthetic apparatus for fatty acid production, the fatty acid synthase (FAS), are considered ideal targets for designing new antibacterial and antimycobacterial agents. The difference between the molecular organization of FAS found in most bacteria/mycobacteria and mammals [1–3] is the reason for this assumption.

Enoyl-acyl reductase (ENR) is a key regulatory step in fatty acid elongation and catalyzes the NADH-dependent stereospecific reduction of  $\alpha,\beta$ -unsaturated fatty acids bound to the acyl carrier protein [4–6].

Biochemical evidence has suggested that isoniazid (INH), a first-line drug for the treatment of tuberculosis, blocks the mycolic acid biosynthesis in *M. tuberculosis*. Mycolic acids are high-molecular-weight  $\alpha$ -alkyl,  $\beta$ -hydroxy fatty acids, which constitute the major components of mycobacterial cell wall [1, 7, 8]. These fatty acids, as well as the key enzyme responsible for their elongation, are considered attractive targets for the rational design of new antituberculosis agents.

The crystal structure of the *M. tuberculosis* enoyl-acyl reductase, InhA, in complex with cofactor nicotinamide adenine dinucleotide (NAD) and the inhibitor INH, was isolated by Rozwarski et al. [9] in 1998 (PDB entry code 1zid). These investigators showed that the drug mechanism of action in *M. tuberculosis* involves a covalent attachment of the activated form of the drug (isonicotinic acyl anion or radical) to the carbon at position 4 of the nicotinamide ring of NAD bound within the active site of InhA, resulting in the formation of an acylpyridine/NAD adduct. The crystal structure of the complex between isonicotinic acyl/NAD and InhA provides a basis for designing new antituberculosis agents that inhibit InhA without needing a KatG drug activation [7, 9].

Previously, we carried out a receptor-independent (RI) 4D-QSAR analysis of a set of 37 INH derivatives (hydrazides) to determine the optimum model and alignment for those compounds [10]. The hypothesized active conformations resulting from (RI) 4D-QSAR analysis can be used as structural design templates, which include their deployment as the molecular geometries of each ligand in structure-based ligand-receptor binding research. Structure-based design (SBD) is the application of ligand-receptor modeling to predict the activity of a

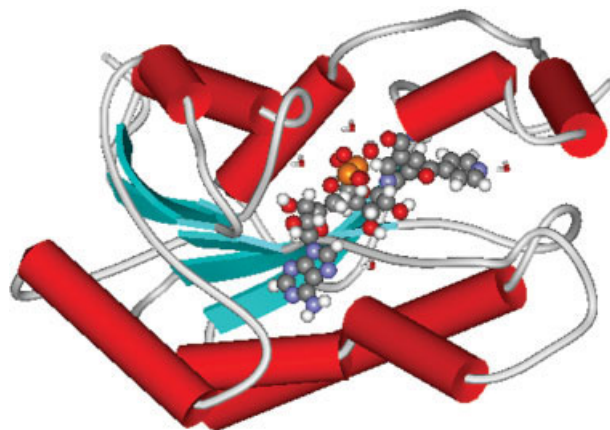


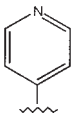
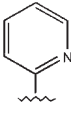
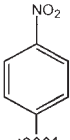
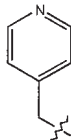
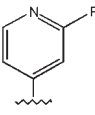
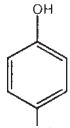
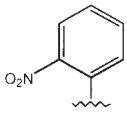
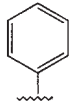
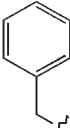
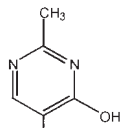
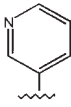
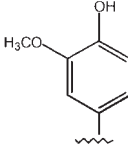
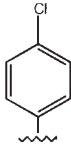
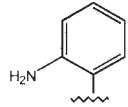
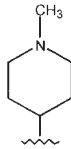
**FIGURE 1.** Schematic representation of InhA in complex with INH/NAD adduct and four water molecules in the active site (ViewerLite 4.2).  $\alpha$ -Helices are presented as red cylinders, and  $\beta$  sheets as cyan flat arrows. The loops are shown as white tubes. The adduct structure is presented in CPK model. Water molecules are shown in stick model. Oxygen atoms are shown in red, nitrogen in blue, carbon atoms in gray, phosphorus in orange, and hydrogen atoms in white. [Color figure can be viewed in the online issue, which is available at [www.interscience.wiley.com](http://www.interscience.wiley.com).]

set of molecules that bind to a common receptor for which the molecular geometry is available.

In the present study, we perform ligand-receptor (L-R) molecular dynamics simulations (MDS) of a set of 16 hydrazides from Ref. [10], including INH, bound to the cofactor NAD in the active site of InhA, the ENR from *M. tuberculosis*. Two models of each ligand (adduct) were docked in the InhA active site to compare the resulting binding thermodynamic descriptors: the hypothesized active conformation from a previous RI 4D-QSAR analysis (set 1a) [10], and the energy-minimized ligand structure without previous treatment (set 1b). Four water solvent molecules that participate in L-R interaction were maintained in the active site during the molecular dynamics (MD) calculations (Fig. 1).

An exploratory data analysis [principal component analysis (PCA)] [11, 12] was carried out to select the most relevant descriptors of the biological activity. The central idea of PCA is to reduce the dimensionality of a data set consisting of a large number of interrelated variables, while retaining as much as possible of the variation present in the data set [11, 12].

**TABLE I**  
Structures and biological activities of the 16 hydrazides.\*

Compound (active, A)	R	pMIC	R—CONHNH <sub>2</sub>		Compound (inactive, I)	R	pMIC	
			Compound (medium activity, M)	R				
INH		4.20						
INHd2		3.82	INHd18		1.92	INHd47		1.00
INHd43		3.40	INHd25		1.92	INHd19		0
INHd14		3.22	INHd30		1.92	INHd41		0.40
INHd37		2.70	INHd27		1.52	INHd48		0.22
INHd15		2.52	INHd22		1.52	INHd49		0.22

INH, isoniazid; INHd, aromatic, heteroaromatic, and ring substituted hydrazides, isoniazid derivatives.

\* Activity was measured as the minimum inhibitory concentration (MIC) against strains of *M. tuberculosis* var. *bovis* at 310 K and given as pMIC (see Refs. [12–15]).

## Methodology

### BUILDING THE MOLECULES AND ATOM CHARGE ASSIGNMENT

A set of 16 hydrazides were randomly selected from Ref. [10] (Table I). Biological activities were evaluated as the minimum inhibitory concentration (MIC;  $\mu\text{g}/\text{mL}$ ), against strains of *M. tuberculosis* var. *bovis* at 310 K [13–16]. The MIC of the compounds was converted to molar units and

then expressed in negative logarithmic units, pMIC ( $-\log \text{MIC}$ ). The pMIC values are given in Table I. The range of activity for the analogues presented in Table I is  $\sim 5$  (0.22–4.70) pMIC units. The set of 16 isoniazid analogues comprises 6 active compounds, including INH [INH, INHd2, INHd43, INHd14, INHd37, INHd15], 5 compounds with medium activity [INHd18, INHd25, INHd30, INHd27, INHd22], and 5 inactive compounds [INHd47, INHd19, INHd41, INHd48, INHd49].

TABLE II

Thermodynamic descriptors from MD simulations and their definitions [22].

Descriptors (Set 1a and 1b)	Definitions of the thermodynamics descriptors
$\Delta E_{\text{stre}} = ELR_{\text{stre}} - EL_{\text{stre}} - ER_{\text{stre}}$	Change in stretching energy upon binding
$\Delta E_{\text{bend}} = ELR_{\text{bend}} - EL_{\text{bend}} - ER_{\text{bend}}$	Change in bending energy upon binding
$\Delta E_{\text{tors}} = ELR_{\text{tors}} - EL_{\text{tors}} - ER_{\text{tors}}$	Change in torsion energy upon binding
$\Delta E_{\text{vdW}} = ELR_{\text{vdW}} - EL_{\text{vdW}} - ER_{\text{vdW}}$	Change in van der Waals energy upon binding
$\Delta E_{\text{el}} = ELR_{\text{el}} - EL_{\text{el}} - ER_{\text{el}}$	Change in electrostatic energy upon binding
$\Delta E_{E1,4} = ELR_{E1,4} - EL_{E1,4} - ER_{E1,4}$	Change in 1-4 interaction energy upon binding
$\Delta E_{\text{Hb}} = ELR_{\text{Hb}} - EL_{\text{Hb}} - ER_{\text{Hb}}$	Change in hydrogen bonding energy upon binding
$\Delta E_{\text{solv}} = ELR_{\text{solv}} - EL_{\text{solv}} - ER_{\text{solv}}$	Change in solvation energy upon binding
$\Delta E_{\text{stre+bend}} = ELR_{\text{stre+bend}} - EL_{\text{stre+bend}} - ER_{\text{stre+bend}}$	Sum of changes in stretching and bending energies
$\Delta E_{\text{stre+bend+tors}} = ELR_{\text{stre+bend+tors}} - EL_{\text{stre+bend+tors}} - ER_{\text{stre+bend+tors}}$	Sum of changes in stretching, bending, and torsion energies
$\Delta E_{\text{el+Hb}} = ELR_{\text{el+Hb}} - EL_{\text{el+Hb}} - ER_{\text{el+Hb}}$	Sum of changes in electrostatic and hydrogen bonding energies
$\Delta E_{\text{el+Hb+E1,4}} = ELR_{\text{el+Hb+E1,4}} - EL_{\text{el+Hb+E1,4}} - ER_{\text{el+Hb+E1,4}}$	Sum of changes in electrostatic, hydrogen bonding, and 1-4 interaction energies
$E_{LR}(\text{LL, RR, LR})$	Ligand-receptor complex energy
$E_{LR}(\text{LR})$	Intermolecular ligand-receptor energy
$E_{LR,\text{vdW}}$	van der Waals intermolecular ligand-receptor energy
$E_{LR,\text{el}}$	Electrostatic intermolecular ligand-receptor energy
$E_{LR,\text{Hb}}$	Hydrogen bonding intermolecular ligand-receptor energy
$E_{LR,\text{el+Hb}}$	Sum of electrostatic and hydrogen bonding intermolecular ligand-receptor energies
$E_{LR,\text{el+Hb+vdW}}$	Sum of electrostatic, hydrogen bonding and van der Waals intermolecular ligand-receptor energies
$\Delta E_L(\text{LL}) = E_{LR}(\text{LL}) - E_L(\text{LL})$	Change in intramolecular ligand energy upon binding
$E_{LR}(\text{LL})$	Intramolecular energy of bound ligand
$E_L(\text{LL})$	Intramolecular energy of unbound ligand
$\Delta E_R(\text{RR}) = E_{LR}(\text{RR}) - E_R(\text{RR})$	Change in intramolecular receptor energy upon binding
$E_{LR}(\text{RR})$	Intramolecular energy of bound receptor
$E_R(\text{RR})$	Intramolecular energy of unbound receptor
$E_{LR}(\text{LRM}) = ELR_{\text{solv}}$	Ligand-receptor complex solvation energy
$\Delta E_L(\text{LM}) = E_{LR}(\text{LM}) - E_L(\text{LM})$	Change in ligand solvation energy upon binding
$E_{LR}(\text{LM})$	Bound ligand solvation energy
$E_L(\text{LM}) = EL_{\text{solv}}$	Unbound ligand solvation energy
$\Delta E_R(\text{RM}) = E_{LR}(\text{RM}) - E_R(\text{RM})$	Change in receptor solvation energy upon binding
$E_{LR}(\text{RM})$	Bound receptor solvation energy
$E_R(\text{RM}) = ER_{\text{solv}}$	Unbound receptor solvation energy

It was assumed that all compounds would act like the lead drug INH, forming an adduct with cofactor NAD in the active site of InhA, as reported by Rozwarski et al. [9]. The ligands of set 1a (the hypothesized active conformations of each of 16 analogues from a previous RI 4D-QSAR analysis) were obtained as reported in Ref. [10]. The three-dimensional (3D) structures of each of the 16 analogues (Table I) of set 1b in their neutral forms were constructed using HyperChem 7.51 software [17]. The crystallized

structure of the isonicotinic acyl/NAD adduct in the active site of the enoyl-acyl reductase from *M. tuberculosis*, InhA (PDB entry code 1zid, 2.7Å resolution), was used as a geometry reference in constructing all ligands. Each structure was energy-minimized using the HyperChem 7.51 MM+ force field without any restriction. The MOLSIM 3.0 program [18] was also used for the optimization of each structure investigated. Partial atomic charges were computed using the AM1 [19] semiempirical method, also implemented in the

HyperChem program [17]. The charges were calculated using the electrostatic potential [17].

As already mentioned, the X-ray structure of the complex InhA-NAD-INH (PDB entry code 1zid, 2.7 Å resolution) was selected as the starting model for the receptor geometry. The 1zid structure has one polypeptide chain or subunit containing 268 amino acid residues and a molecular weight of 28,352 Da. Both the N-terminus and C-terminus were modeled as neutral, and the CH<sub>3</sub> groups were used as the block groups. AMBER [20] partial charges were assigned to all atoms of the enzyme structure, except the block groups, using the HyperChem 7.51 program [17]. The charge state of ionizable residues was modeled at neutral pH. Lone pair electrons were not modeled explicitly. Only four water solvent molecules that participate in the L-R interaction [9] were maintained in the InhA active site model. The MOLSIM 3.2 program [18] was used to perform the energy minimization of the modeled InhA-NAD-INH complex. The energy-minimized structure of the complex was used as the initial structure in the MD calculations (item 2).

### MOLECULAR DYNAMICS PROCEDURE

Energy minimization and MD calculations were performed using the MOLSIM program, version 3.2 [18]. The hydration shell model proposed by Hopfinger [21] was included in the force field representation to estimate aqueous solvation energies. Solvation energy and hydrogen bonding energy contributions were evaluated only for the lowest-energy structures. The molecular dielectric constant was set to a value of 3.5. The simulation temperature was set to a value of 310 K, the same used in the biological assay [13–16]. An average temperature of 310 K was held constant during the simulation by coupling the system to a temperature external bath with a relaxation time of 0.01 ps [22].

The energy-minimized structure of the InhA-NAD-INH complex was used as the initial structure in MD calculations. The MDS [23] protocol employed 500,000 steps with a step size of 0.001 ps (1 fs) at 310 K. An output trajectory file was saved every 20 simulation steps, resulting in 25,000 conformations. The solvation energy of the lowest-energy conformation obtained by MDS was calculated using the hydration shell model [20]. The lowest-energy conformation of the InhA-NAD-INH model was used to dock the energy-optimized structures of all ligands (adducts from the two sets, 1a and 1b), employing the optimum model/align-

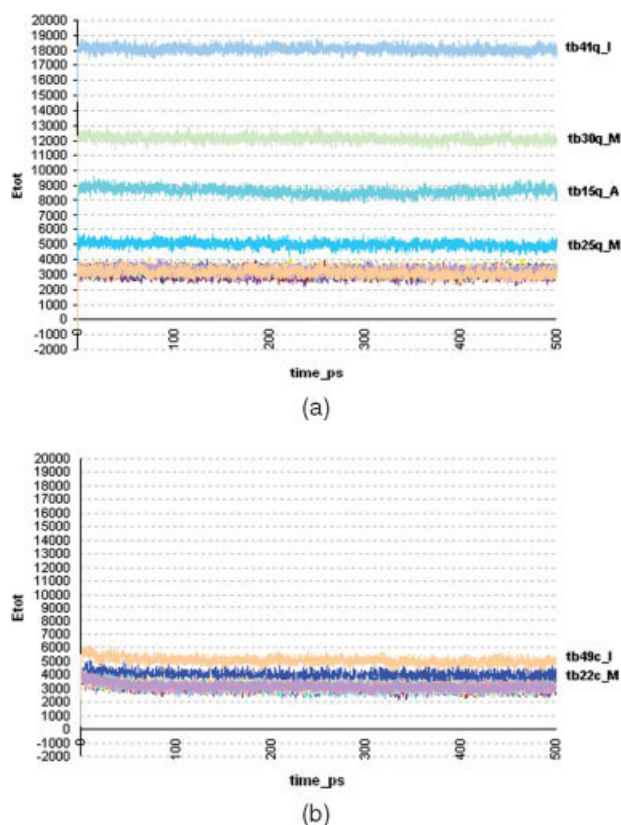


**FIGURE 2.** (a) Total energy ( $E_{\text{tot}}$ , kcal/mol) plotted versus time (ps) from MDS of the L-R complexes (set 1a).  $E_{\text{tot}}$  corresponds to the descriptor  $E_{\text{LR}}(\text{LL}, \text{RR}, \text{LR})$ .  $E_{\text{LR}}(\text{LL}, \text{RR}, \text{LR}) = \text{ELR}_{\text{stre}} + \text{ELR}_{\text{bend}} + \text{ELR}_{\text{tors}} + \text{ELR}_{\text{E1,4}} + \text{ELR}_{\text{vdW}} + \text{ELR}_{\text{el}} + \text{ELR}_{\text{vdW+el}} + \text{ELR}_{\text{Hb}} + E_{\text{LR}}(\text{LRM})$  (Table III). (b) Total energy ( $E_{\text{tot}}$ , kcal/mol) plotted versus time (ps) from MDS of the L-R complexes (set 1b).  $E_{\text{tot}}$  corresponds to the descriptor  $E_{\text{LR}}(\text{LL}, \text{RR}, \text{LR})$ .  $E_{\text{LR}}(\text{LL}, \text{RR}, \text{LR}) = \text{ELR}_{\text{stre}} + \text{ELR}_{\text{bend}} + \text{ELR}_{\text{tors}} + \text{ELR}_{\text{E1,4}} + \text{ELR}_{\text{vdW}} + \text{ELR}_{\text{el}} + \text{ELR}_{\text{vdW+el}} + \text{ELR}_{\text{Hb}} + E_{\text{LR}}(\text{LRM})$  (Table V). [Color figure can be viewed in the online issue, which is available at [www.interscience.wiley.com](http://www.interscience.wiley.com).]

ment selected in Ref. [10] (HyperChem 7.51). The energy-minimized structure of each InhA-NAD-analogue complex (sets 1a and 1b) was used to perform MDS of 500 ps (step size, 1 fs) at 310 K, and an output trajectory file was recorded every 20 simulation steps. The solvation energy and hydrogen bonding energy contributions of the lowest-energy conformation from the MDS of each InhA-NAD-analogue model (sets 1a and 1b) (L-R bound state) were calculated. At this point, the L-R bound-state thermodynamic descriptors were generated.

The INH/NAD adduct was extracted from the lowest-energy conformation of the InhA-NAD-

**TABLE III**  
**Thermodynamic descriptors found for the L-R lowest-energy conformations (set 1a) from 500 ps MDS at 310 K.**

Complex L-R	ELR <sub>site</sub> (kcal · mol)	ELR <sub>bind</sub> (kcal · mol)	ELR <sub>tors</sub> (kcal · mol)	ELR <sub>E1.4</sub> (kcal · mol)	ELR <sub>vdw</sub> (kcal · mol)	ELR <sub>el-Hb-vdw</sub> (kcal · mol)	ELR <sub>el</sub> (kcal · mol)	ELR <sub>vdw+el</sub> (kcal · mol)	ELR <sub>hb</sub> (kcal · mol)	E <sub>LR(LRM)</sub> (kcal · mol)	E <sub>LR(LL, RR, LR)</sub> (kcal · mol)
tb1q_A	1469.54	2781.40	2172.69	4815.92	-2047.73	-6599.26	-210.44	-42474.01	-13.26	-40105.15	
tb2q_A	1522.07	2759.81	2154.09	4753.68	-2015.60	-6584.91	-268.93	-41645.92	-16.60	-39342.31	
tb14q_A	1500.04	2823.15	2154.49	4868.65	-1938.66	-6624.75	-153.83	-43358.81	-16.19	-40745.90	
tb43q_A	1470.41	2836.84	2156.84	4881.32	-2043.78	-6890.78	-146.71	-42452.82	-27.30	-40215.97	
tb37q_A	1471.59	2847.20	2166.10	4817.33	-2088.99	-6701.81	-278.96	-42573.21	-30.21	-40370.96	
tb15q_A	1413.49	2907.01	2213.36	4754.11	668.03	-6725.55	2518.88	-42084.63	-2.45	-34337.76	
SD	36.57	51.98	22.66	54.31	1101.36	114.21	1116.16	569.16	10.04	2419.63	
tb18q_M	1464.14	2853.29	2166.61	5036.75	-2055.80	-6711.67	-257.30	-43057.93	-39.28	-40601.18	
tb25q_M	2397.06	2807.40	2178.95	4936.98	-1540.81	-6852.86	282.84	-41246.37	-27.00	-37063.82	
tb30q_M	1554.58	2825.03	2137.75	4942.77	-2375.99	-6804.59	4293.50	-41953.53	-29.04	-30657.54	
tb22q_M	1484.35	2722.86	2241.81	4967.91	-2046.40	-6784.48	-121.81	-42750.15	-24.27	-40310.18	
tb27q_M	1540.32	2781.67	2166.76	4940.66	-2024.18	-6560.16	-285.67	-42547.47	-19.95	-40008.02	
SD	398.11	49.47	38.56	41.92	1932.06	114.01	1975.90	719.01	7.21	4199.82	
tb47q_I	1506.48	2823.75	2200.46	4929.07	-2095.58	-6785.09	-182.86	-44163.64	-44.54	-41811.95	
tb19q_I	1397.92	2771.69	2193.55	4908.63	-2015.11	-6662.29	-136.27	-42934.78	-16.36	-40493.02	
tb41q_I	1517.90	2767.99	2160.66	4957.61	5383.59	-6585.88	7221.54	-43200.27	-22.27	-25799.13	
tb48q_I	1482.69	2795.52	2174.46	4989.05	-2058.92	-6666.27	-179.47	-41771.38	-25.24	-39259.56	
tb49q_I	1445.80	2801.13	2190.53	4876.44	-2073.55	-6763.61	-223.45	-43719.60	-30.99	-41497.30	
SD	48.91	22.87	16.13	43.45	3329.36	81.54	3310.44	908.44	10.70	6766.93	

Complex L-R	E <sub>LR(LR)</sub> (kcal · mol)	E <sub>LR(vdw)</sub> (kcal · mol)	E <sub>LR(el)</sub> (kcal · mol)	E <sub>LR(el+Hb)</sub> (kcal · mol)	E <sub>LR(el+Hb+vdw)</sub> (kcal · mol)	E <sub>LR(LL)</sub> (kcal · mol)	E <sub>LR(RR)</sub> (kcal · mol)	E <sub>LR(LM)</sub> (kcal · mol)	E <sub>LR(RM)</sub> (kcal · mol)
tb1q_A	10314.92	-157.18	-305.13	-42579.14	-42736.32	-259.56	11499.10	-5.17	-8.10
tb2q_A	10116.17	-145.68	-391.05	-42036.97	-42182.65	-275.51	11465.14	-3.62	-12.98
tb14q_A	11125.33	51.88	-162.38	-43521.19	-43469.31	-203.50	11549.83	-3.13	-13.06
tb43q_A	10694.15	-160.92	-164.70	-42617.52	-42778.44	-191.25	11536.64	-4.82	-22.49
tb37q_A	10556.61	-139.70	-233.10	-42806.31	-42479.81	-285.34	11587.55	-5.02	-25.19
tb15q_A	21805.09	5363.34	-104.78	-42189.41	-36826.07	-310.99	11598.96	-3.72	1.26
SD	4603.14	2236.10	105.88	524.16	2447.50	47.35	51.23	0.86	9.64
tb18q_M	10556.25	-163.08	-319.18	-43377.11	-43540.19	-67.72	11588.49	-9.14	-30.13
tb25q_M	13445.58	776.26	-213.66	-41460.03	-40683.77	155.63	12164.75	-3.96	-23.05
tb30q_M	28828.91	8767.28	-82.88	-42036.41	-33269.13	-96.96	11557.07	-7.03	-22.01
tb22q_M	10952.67	-149.33	-82.80	-42832.95	-42982.28	-113.36	11530.29	-4.78	-19.49
tb27q_M	10982.68	-160.54	-62.82	-42610.29	-42770.83	-92.40	11521.80	-4.36	-15.57
SD	7840.77	3907.92	110.98	738.59	4265.24	112.21	276.42	2.19	5.36
tb47q_I	10887.99	-156.32	-129.56	-44293.20	-44449.52	-118.54	11578.29	-6.90	-37.63
tb19q_I	7123.78	-132.28	-171.06	-43238.12	-43238.12	-82.36	11570.86	-8.22	-8.13
tb41q_I	4018.08	14700.70	-308.74	-43509.01	-28808.31	-113.97	11518.13	-2.40	-19.87
tb48q_I	11266.92	-168.90	81.50	-41689.88	-41858.78	-71.99	11513.71	-4.36	-20.88
tb49q_I	10356.65	-165.08	-313.54	-44033.14	-44198.19	-192.85	11506.74	-1.92	-29.07
SD	13640.26	6643.97	161.81	1024.01	6620.31	47.39	34.15	2.75	11.03

A, active; M, medium activity; I, inactive; q, ligands from (Rf) 4D-QSAR [10] (adduct INH analogue/NAD); tb, antituberculosis complexes (InhA-adduct INH analogue/NAD); SD, standard deviation of the descriptors found for the L-R lowest-energy conformations from MDS, regarding the biological activity class.

TABLE IV

Thermodynamic descriptors found for the L lowest-energy conformations (set 1a) from 500 ps MDS at 310 K.

Ligand (L)	$E_{L_{\text{stre}}}$ (kcal · mol)	$E_{L_{\text{bend}}}$ (kcal · mol)	$E_{L_{\text{tors}}}$ (kcal · mol)	$E_{L_{E_{1,4}}}$ (kcal · mol)	$E_{L_{\text{vdW}}}$ (kcal · mol)	$E_{L_{\text{el}}}$ (kcal · mol)	$E_{L_{\text{Hb}}}$ (kcal · mol)	$E_L(\text{LM})$ (kcal · mol)	$E_L(\text{LL})$ (kcal · mol)
INHq_A	22.78	64.32	19.21	-431.46	-15.33	100.30	-227.17	-14.54	-481.89
INHd2q_A	33.04	60.61	18.83	-430.10	-16.57	97.82	-213.63	-16.15	-466.14
INHd14q_A	36.02	59.23	17.38	-404.22	-10.05	72.63	-208.71	-14.48	-452.20
INHd43q_A	28.63	66.67	21.30	-416.26	-21.04	87.15	-246.12	-13.41	-493.07
INHd37q_A	30.54	56.77	19.28	-445.08	-15.14	105.30	-243.96	-14.02	-506.32
INHd15q_A	23.09	64.01	18.65	-463.33	-15.30	107.85	-196.23	-16.91	-478.17
SD	5.32	3.69	1.27	20.86	3.51	13.18	20.00	1.33	19.16
INHd18q_M	31.76	56.52	18.75	-238.38	-13.31	28.10	-203.67	-20.71	-340.94
INHd25q_M	26.76	55.20	19.93	-265.73	-16.72	47.97	-225.83	-17.33	-375.75
INHd30q_M	28.05	59.17	13.00	-270.64	-18.35	58.68	-224.62	-15.83	-370.54
INHd22q_M	31.53	58.83	23.04	-280.71	-23.26	51.05	-293.67	-14.58	-447.77
INHd27q_M	31.34	62.12	16.83	-277.33	-17.51	48.98	-258.21	-13.29	-407.06
SD	2.32	2.66	3.73	16.79	3.59	11.35	35.22	2.86	40.63
INHd47q_I	24.56	64.36	14.39	-273.19	-22.93	38.39	-203.01	-12.59	-370.02
INHd19q_I	26.75	65.82	30.74	-271.62	-19.74	58.64	-225.78	-16.54	-351.73
INHd41q_I	19.49	64.84	18.83	-268.73	-17.34	36.58	-237.45	-15.27	-399.05
INHd48q_I	34.98	60.83	25.84	-262.96	-26.54	48.80	-263.32	-11.69	-394.06
INHd49q_I	25.55	69.42	28.45	-396.95	-22.57	86.27	-352.62	-8.60	-571.05
SD	5.60	3.08	6.84	57.30	3.48	20.23	57.99	3.12	88.10

A, active; M, medium activity; I, inactive; q, ligands from (RI) 4D-QSAR analysis [10]; SD, standard deviation of the descriptors found for the L lowest-energy conformations from MDS, regarding the biological activity class; INH, isoniazid; INHd, aromatic, heteroaromatic, and ring substituted hydrazides, isoniazid derivatives.

INH complex (HyperChem 7.51) [17], and the InhA model without the INH/NAD adduct was employed to obtain the thermodynamic descriptors of the receptor unbound state (R unbound state). The energy-minimized structure of the InhA model without the INH/NAD adduct was used as the initial structure to perform MDS of 500 ps at 310 K, as already described. The solvation energy and hydrogen bonding energy contributions of the R lowest-energy conformation obtained from MDS were calculated, and the R unbound-state thermodynamic descriptors were generated.

Likewise, the thermodynamic descriptors of each ligand (L) (sets 1a and 1b) in its unbound state were generated. The lowest-energy conformation of each InhA–NAD–analogue model from MDS was used to extract the adduct, analogue/NAD (HyperChem 7.51) [17]. The energy-minimized structure of each adduct model (sets 1a and 1b) was employed as initial structure to perform MDS of 500 ps at 310 K. The solvation energy and hydrogen bonding energy contributions of each L lowest-energy conformation from MDS were calculated.

The thermodynamic descriptors from MD calculations and their respective definitions [24] are presented in Table II. A preliminary PCA [11, 12] was

employed to explore the data considering the most relevant descriptors (independent variables) of the biological activity.

## Results and Discussion

The range of the L-R complex energy [ $E_{L,R}(\text{LL}, \text{RR}, \text{LR})$ ] from MDS is distinct to four L-R complexes of set 1a: tb15q\_A, tb25q\_M, tb30q\_M, and tb41q\_I, as represented in Figure 2(a). Otherwise, the L-R complexes of set 1b did not present significant changes in the  $E_{L,R}(\text{LL}, \text{RR}, \text{LR})$  range from MDS [Fig. 2(b)].  $E_{L,R}(\text{LL}, \text{RR}, \text{LR})$  corresponds to the summation of the following L-R complex energy (ELR) contributions: stretching energy ( $ELR_{\text{stre}}$ ), bending energy ( $ELR_{\text{bend}}$ ), torsion energy ( $ELR_{\text{tors}}$ ), Lennard-Jones or 1,4 interactions energy ( $ELR_{E_{1,4}}$ ), intramolecular van der Waals energy ( $ELR_{\text{vdW}}$ ), intramolecular electrostatic energy ( $ELR_{\text{el}}$ ), sum of intermolecular van der Waals and electrostatic energies ( $ELR_{\text{vdW}+\text{el}}$ ), hydrogen bonding energy ( $ELR_{\text{Hb}}$ ), and solvation energy ( $E_{L,R}(\text{LRM})$ ). The  $ELR_{\text{vdW}+\text{el}}$  positive values found for the complexes tb15q\_A, tb25q\_M, tb30q\_M, and tb41q\_I (see Table III), can be attributed to the van der Waals intermo-

**TABLE V**  
**Thermodynamic descriptors found for the L-R lowest-energy conformations (set 1b) from 500 ps MDS at 310 K.**

Complex L-R	ELR <sub>stre</sub> (kcal · mol)	ELR <sub>bend</sub> (kcal · mol)	ELR <sub>tors</sub> (kcal · mol)	ELR <sub>E1.4</sub> (kcal · mol)	ELR <sub>vdw</sub> (kcal · mol)	ELR <sub>el</sub> (kcal · mol)	ELR <sub>vdw+el</sub> (kcal · mol)	ELR <sub>Hb</sub> (kcal · mol)	E <sub>LR(LRM)</sub> (kcal · mol)	E <sub>LR(LL, RR, LR)</sub> (kcal · mol)
tb1c_A	1496.24	2768.98	2185.43	4955.93	-2047.09	-6731.72	-163.27	-41927.08	-18.10	-39480.68
tb2c_A	1554.21	2775.87	2159.53	4805.82	-2064.80	-6604.33	-320.26	-42148.44	-45.28	-39887.68
tb14c_A	1494.76	2802.99	2191.46	4815.60	-2071.49	-6690.76	-258.88	-43125.22	-40.48	-40846.55
tb43c_A	1482.24	2819.83	2226.99	5001.36	-2030.93	-6807.01	-271.22	-42782.13	-13.31	-40510.61
tb37c_A	1539.65	2801.46	2172.24	4859.57	-2115.71	-6825.60	-208.12	-43265.21	-53.94	-41070.16
tb15c_A	1350.02	2807.34	2117.21	4833.47	-2022.13	-6472.55	-231.49	-41720.14	-28.94	-39392.21
SD	72.41	19.55	36.52	50.85	33.75	132.99	54.26	650.52	15.97	712.62
tb18c_M	1468.65	2801.56	2147.91	4952.82	-2063.15	-6607.80	-368.15	-41949.42	-32.82	-39650.40
tb25c_M	1512.88	2809.87	2143.75	4815.60	-2027.43	-6694.18	-315.69	-40788.36	-26.33	-38569.89
tb30c_M	1493.65	2820.04	2157.51	5001.36	-2059.29	-6813.41	-144.40	-42057.54	-11.45	-39613.52
tb22c_M	1678.06	2894.81	2272.00	4903.00	-1904.09	-6716.90	-219.60	-41678.00	-15.74	-38786.46
tb27c_M	1443.76	2793.71	2160.87	4827.24	-2069.58	-6712.03	-225.46	-43134.18	-34.10	-40949.76
SD	92.43	40.78	53.89	79.83	69.36	73.20	87.81	841.60	10.14	936.83
tb47c_I	1502.72	2856.67	2133.71	4899.51	-2050.87	-6821.50	-118.38	-43027.50	-17.67	-40643.31
tb19c_I	1513.37	2846.31	2165.98	4811.23	-2042.57	-6780.55	-258.32	-41698.50	-11.56	-39454.61
tb41c_I	1457.89	2759.14	2214.83	4859.67	-2049.33	-6709.59	-279.74	-42911.22	-14.13	-40672.48
tb48c_I	1501.63	2752.00	2191.13	4904.87	-2005.74	-6657.87	-230.54	-40620.91	-45.37	-38210.80
tb49c_I	2350.96	2916.35	2144.21	4890.66	-1582.21	-6761.04	258.05	-42029.74	-50.56	-37863.32
SD	383.88	69.75	33.37	38.81	204.27	63.66	223.40	982.75	18.57	1317.08
Complex L-R	E <sub>LR(LR)</sub> (kcal · mol)	E <sub>LR,vdw</sub> (kcal · mol)	E <sub>LR,el</sub> (kcal · mol)	E <sub>LR,el+Hb</sub> (kcal · mol)	E <sub>LR,el+Hb+vdw</sub> (kcal · mol)	E <sub>LR(LL)</sub> (kcal · mol)	E <sub>LR(RR)</sub> (kcal · mol)	E <sub>LR(LM)</sub> (kcal · mol)	E <sub>LR(RM)</sub> (kcal · mol)	
tb1c_A	10742.62	-162.32	-169.66	-42096.74	-42259.06	-82.54	11489.12	-5.54	-12.56	
tb2c_A	10221.11	-143.98	-393.17	-42541.61	-42685.59	-213.07	11508.48	-3.79	-41.48	
tb14c_A	10549.72	-180.36	-214.92	-43340.14	-43520.50	-205.56	11545.84	-2.49	-38.00	
tb43c_A	10312.94	-180.56	-359.96	-43142.09	-43322.65	-201.60	11595.58	-5.20	-8.10	
tb37c_A	10753.27	-183.36	-126.46	-43391.67	-43575.03	-189.18	11562.09	-3.64	-24.79	
tb15c_A	10082.27	-148.24	-364.64	-42084.78	-42233.02	-205.85	11313.88	-5.04	-48.90	
SD	280.61	17.50	114.82	604.13	618.80	49.82	99.89	1.17	16.48	
tb18c_M	10187.64	-189.46	-402.18	-42351.60	-42541.06	-179.94	11550.86	-7.86	-24.95	
tb25c_M	10176.88	-162.44	-390.16	-41178.52	-41340.96	-207.11	11489.19	-4.09	-22.24	
tb30c_M	10614.16	-180.18	-249.00	-42306.54	-42486.72	-116.89	11589.41	-4.03	-10.07	
tb22c_M	10971.26	-169.68	-218.62	-41896.62	-42066.30	-209.59	11957.45	-1.69	-14.05	
tb27c_M	10523.05	-154.56	-196.70	-43330.88	-43485.44	-182.31	11407.88	-7.76	-26.33	
SD	330.71	13.87	97.58	782.28	780.59	37.40	211.83	2.67	7.11	
tb47c_I	10713.17	-157.72	-182.00	-43209.50	-43367.22	-114.83	11507.44	-8.85	-8.82	
tb19c_I	10303.55	-171.10	-345.56	-42044.06	-42215.16	-196.81	11533.68	-3.79	-7.76	
tb41c_I	10237.32	-138.10	-389.00	-43438.32	-43438.32	-220.55	11512.07	-5.24	-8.88	
tb48c_I	10549.10	-146.72	-253.54	-41021.17	-41021.17	-191.83	11541.45	-7.49	-37.87	
tb49c_I	13798.96	766.70	-18.30	-42048.04	-41281.34	451.54	11850.62	-5.95	-44.61	
SD	1509.47	411.67	146.64	998.59	1130.13	285.66	146.92	1.97	18.10	

A, active; M, medium activity; I, inactive; c, ligands built from crystallographic structure 1zid [9] without previous treatment (adduct INH analogue/NAD); tb, antituberculosis complexes (InhA-adduct INH analogue/NAD); SD, standard deviation of the descriptors found for the L-R lowest-energy conformations from MDS, regarding the biological activity class.

TABLE VI

Thermodynamic descriptors found for the L lowest-energy conformations (set 1b) from 500 ps MDS at 310 K.

Ligand (L)	$E_{L_{\text{stre}}}$ (kcal · mol)	$E_{L_{\text{bend}}}$ (kcal · mol)	$E_{L_{\text{tors}}}$ (kcal · mol)	$E_{L_{E1,4}}$ (kcal · mol)	$E_{L_{\text{vdW}}}$ (kcal · mol)	$E_{L_{\text{el}}}$ (kcal · mol)	$E_{L_{\text{Hb}}}$ (kcal · mol)	$E_L(\text{LM})$ (kcal · mol)	$E_L(\text{LL})$ (kcal · mol)
INHc_A	32.31	63.86	16.93	-308.54	-16.44	33.95	-236.92	-14.71	-429.55
INHd2c_A	25.97	59.65	17.48	-429.55	-18.31	80.56	-262.39	-13.00	-539.59
INHd14c_A	33.19	64.24	17.91	-428.73	-18.49	87.29	-241.25	-13.42	-499.26
INHd43c_A	25.04	60.18	15.26	-420.71	-11.80	75.14	-301.76	-12.57	-571.22
INHd37c_A	32.20	62.14	17.69	-434.64	-14.90	91.22	-249.35	-15.10	-510.74
INHd15c_A	30.67	61.56	15.62	-423.14	-18.24	82.73	-208.38	-15.66	-474.83
SD	3.51	1.87	1.12	48.76	2.64	20.93	31.03	1.25	49.49
INHd18c_M	35.03	73.72	20.48	-386.53	-19.17	73.59	-203.23	-17.92	-424.03
INHd25c_M	25.22	64.40	20.08	-392.45	-21.37	92.46	-286.71	-13.20	-511.57
INHd30c_M	24.10	62.39	15.58	-277.42	-21.30	49.02	-272.11	-11.50	-431.23
INHd22c_M	25.99	59.72	20.30	-406.08	-22.60	64.43	-274.19	-14.75	-547.18
INHd27c_M	27.10	63.84	27.38	-383.09	-22.70	81.09	-263.90	-15.00	-485.28
SD	4.36	5.30	4.23	52.00	1.42	16.50	32.78	2.38	52.56
INHd47c_I	33.99	52.62	14.05	-281.55	-24.10	37.93	-213.33	-14.38	-394.76
INHd19c_I	35.54	62.16	22.45	-376.59	-11.12	71.42	-232.48	-18.21	-446.83
INHd41c_I	25.88	67.78	20.57	-415.06	-19.53	88.32	-285.94	-13.68	-531.66
INHd48c_I	28.25	63.01	26.76	-382.75	-20.43	97.29	-288.00	-13.09	-488.97
INHd49c_I	24.15	72.18	30.17	-396.50	-23.37	73.85	-259.75	-11.30	-490.57
SD	5.00	7.32	6.16	51.87	5.17	22.67	32.82	2.55	51.92

A, active; M, medium activity; I, inactive; c, ligands built from crystallographic structure 1zid [9] without previous treatment; SD, standard deviation of the descriptors found for the L lowest-energy conformations from MDS, regarding the biological activity class; INH, isoniazid; INHd, aromatic, heteroaromatic, and ring substituted hydrazides, isoniazid derivatives.

lecular L-R energy ( $E_{L_{R,\text{vdW}}}$ ) rather than to the electrostatic intermolecular L-R energy ( $E_{L_{R,\text{el}}}$ ). Thus, the  $E_{L_{R,\text{vdW}}}$  contribution in  $E_{L_{R,\text{vdW}+\text{el}}}$  is probably responsible for the difference in the  $E_{L_{R}}(\text{LL}, \text{RR}, \text{LR})$  range observed in Figure 2(a). The  $E_{L_{R}}(\text{LL}, \text{RR}, \text{LR})$  values found for each L-R lowest-energy conformation of sets 1a and 1b are shown in Tables III and V, respectively.

The thermodynamic descriptors of the bound and unbound states found for the set 1a and 1b are presented in Tables III–VII. As already mentioned, those descriptors were generated for the lowest energy conformation of each L-R state from MD calculations (500 ps at 310 K).

Each data set was organized in a matrix format composed of 16 rows (investigated ligands) and 66

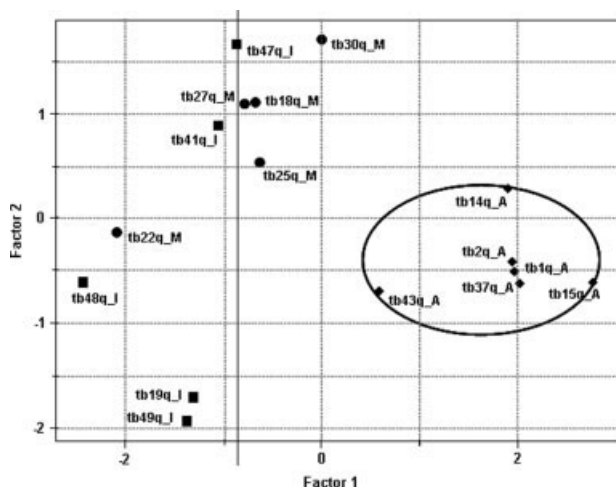
columns (independent variables = thermodynamic descriptors) (see Table II). The correlation coefficients between the independent variables (descriptors) from MDS and biological activity data (pMIC) suggest that the following energy contributions are important to set 1a: 1-4 interaction energy (Lennard-Jones) of the complex L-R [ $E_{L_{R,E1,4}}$ ] (-0.62); 1-4 bonding energy (Lennard-Jones) of unbound L [ $E_{L_{E1,4}}$ ] (-0.67); van der Waals bonding energy of unbound L [ $E_{L_{\text{vdW}}}$ ] (0.60); electrostatic bonding energy of unbound L [ $E_{L_{\text{el}}}$ ] (0.63); and the sum of electrostatic and hydrogen bonding energies of unbound L [ $E_{L_{\text{el}+\text{Hb}}}$ ] (0.73). Likewise, the dihedral torsional energy of unbound L [ $E_{L_{\text{tors}}}$ ] appears to be relevant to the biological activity in set 1b (-0.62).

TABLE VII

Thermodynamic descriptors found for the R lowest-energy conformation from 500 ps MDS at 310 K.

Receptor (R)	$E_{R_{\text{stre}}}$ (kcal · mol)	$E_{R_{\text{bend}}}$ (kcal · mol)	$E_{R_{\text{tors}}}$ (kcal · mol)	$E_{R_{E1,4}}$ (kcal · mol)	$E_{R_{\text{vdW}}}$ (kcal · mol)	$E_{R_{\text{el}}}$ (kcal · mol)	$E_{R_{\text{vdW}+\text{el}}}$ (kcal · mol)	$E_{R_{\text{Hb}}}$ (kcal · mol)	$E_R(\text{RM})$ (kcal · mol)	$E_R(\text{RR})$ (kcal · mol)
InhA	1444.53	2716.74	2114.78	5202.71	-2010.33	-6927.25	-46.60	-43175.74	-20.23	-40701.39

InhA model, enoyl-acyl reductase from *M. tuberculosis*.



**FIGURE 3.** Scores plot obtained for set 1a employing PCA. The Factor 1 or PC1 discriminates the active ligands (solid losangles) from the ligands with medium activity (solid circles) and inactive ligands (solid squares).

Comparing all descriptors obtained for set 1a with the respective descriptors of set 1b, the correlation value was 0.9959, which points to the conclusion that there is no significant difference between the two data sets. Therefore, in this study, only the results of exploratory analysis (PCA) found for set 1a, which contains the hypothesized active conformations from a previous RI 4D-QSAR analysis [10], are discussed.

Through PCA, the principal component 1 (PC1) or Factor 1 is related to the biological activity data. PC1 discriminates the active complexes of set 1a, as presented in the scores plot (Fig. 3). The active complexes are located at the right side of the scores diagram (with positive scores in PC1), whereas medium activity appears to be more in the center, and inactive complexes at the left side (exception is tb22q\_M). The descriptors responsible for that behavior can be seen in the loadings plot (Fig. 4). The 1-4 bonding energy (Lennard-Jones) of unbound L [ $EL_{E1,4}$ ] and the dihedral torsional energy of unbound L [ $EL_{tors}$ ] contribute negatively to the biological activity, whereas the van der Waals bonding energy of unbound L [ $EL_{vdW}$ ], the electrostatic bonding energy of unbound L [ $EL_{el}$ ], and the sum of electrostatic and hydrogen bonding energies of unbound L [ $EL_{el+Hb}$ ] have a positive influence on the biological activity. In this study, the MDS of the unbound L state generated the principal energy contributions to the biological activity. The main

difference among medium active and inactive complexes is the  $EL_{E1,4}$  and  $EL_{tors}$  contributions.  $EL_{E1,4}$  values appear to be higher for medium active ligands, and the  $EL_{tors}$  contribution is probably minor for inactive ligands (see Table IV).

The descriptors that probably decrease the biological activity,  $EL_{E1,4}$  and  $EL_{tors}$ , are related to the ligand intramolecular interactions. The increase of those energies means that the ligand intramolecular bonds are more present (ligand more bent), impairing some intermolecular interactions with the amino acid residues in the InhA active site. Otherwise, the descriptors responsible for increasing biological activity ( $EL_{vdW}$ ,  $EL_{el}$ , and  $EL_{el+Hb}$ ) appear to be related to the intermolecular interactions present in the hydrophobic pocket of the InhA active site, which is formed by hydrophobic residues (Phe149, Gly192, Pro193, Leu218, Tyr158, and Trp222) [9], as well as the intermolecular interactions with polar amino acid residues and water molecules, which participate in L-R interactions in the active site.

## Conclusions

The thermodynamic descriptors ( $EL_{E1,4}$ ,  $EL_{tors}$ ,  $EL_{vdW}$ ,  $EL_{el}$ , and  $EL_{el+Hb}$ ) were selected simply using their correlation coefficient with the biological activity. These independent variables provided a satisfactory interpretation of the data set, as shown by PCA. The next step is the construction of QSAR models, considering the selected thermodynamic descriptors. When the number of analogues (observations) is small compared with the number

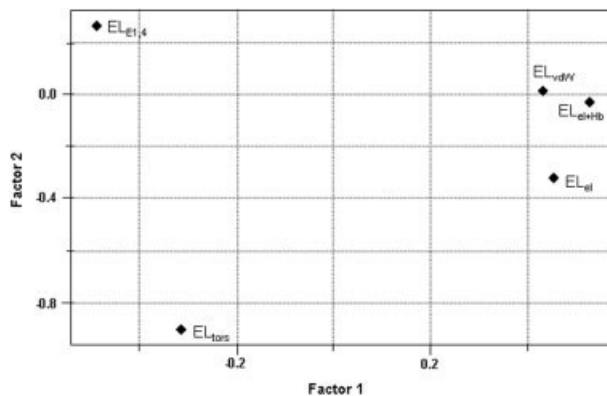


**FIGURE 4.** Loadings plot found for set 1a using PCA. The relevant descriptors to the biological activity are  $EL_{E1,4}$ ,  $EL_{tors}$ ,  $EL_{vdW}$ ,  $EL_{el}$ , and  $EL_{el+Hb}$ .

of independent variables (thermodynamic descriptors), and many of the energy terms are interrelated to one another, the “funnel” strategy for optimizing the construction of QSAR models is the genetic function algorithm (GFA) [25]. The resulting QSAR models could be compared with QSAR models generated by other methods, as the GFA optimization method.

### ACKNOWLEDGMENTS

K. F. M. P. is grateful to CNPq for scholarship support, to FAPESP to financial support, and to the Chem21 Group, for providing the license of MOLSIM 3.2 program used in this study.

---

### References

- Barry, C. E., III; Lee, R. E.; Mdluli, K.; Sampson, A. E.; Schroeder, B. G.; Slayden, R. A.; Yuan, Y. *Prog Lipid Res* 1998, 37, 143.
- McCarthy, A. D.; Hardie, D. G. *Trends Biochem* 1984, 9, 60.
- Magnuson, K.; Jackowski, S.; Rock, C. O.; Cronan, J. E., Jr. *Microbiol Rev* 1993, 57, 522.
- Bergler, H.; Fuchsbichler, S.; Högenauer, G.; Turnowsky, F. *Eur J Biochem* 1996, 242, 689.
- Stewart, M.; Parikh, S.; Xiao, G.; Tonge, P. J.; Kisker, C. *J Mol Biol* 1999, 290, 859.
- Rozwarski, D. A.; Vilchèza, C.; Sugantino, M.; Bittman, R.; Sacchettini, J. C. *J Biol Chem* 1999, 274, 15582.
- Pasqualoto, K. F. M.; Ferreira, E. I. *Curr Drug Targets* 2001, 2, 427.
- Brenan, P. J.; Nikaido, H. *Annu Rev Biochem* 1995, 64, 29.
- Rozwarski, D. A.; Grant, G. A.; Barton, D. H. R.; Jacobs, W. R., Jr.; Sacchettini, J. C. *Science* 1998, 279, 98.
- Pasqualoto, K. F. M.; Ferreira, E. I.; Santos-Filho, O. A.; Hopfinger, A. J. *J Med Chem* 2004, 47, 3755.
- Jolliffe, I. T. *Springer Series in Statistics—Principal Components Analysis*; 2nd ed.; Springer-Verlag: New York, 2002.
- Beebe, K. R.; Pell, R. J.; Seasholtz, M. B. *Chemometrics: A Practical Guide*; Wiley: New York, 1998.
- Bernstein, J.; Lott, W. A.; Steinberg, B. A.; Yale, H. L. *Am Rev Tuberc* 1952, 65, 357.
- Bernstein, J.; Jambor, W. P.; Lott, W. A.; Pansy, F.; Steinberg, B. A.; Yale, H. L. *Am Rev Tuberc* 1953, 67, 354.
- Bernstein, J.; Jambor, W. P.; Lott, W. A.; Pansy, F.; Steinberg, B. A.; Yale, H. L. *Am Rev Tuberc* 1953, 67, 366.
- Klopman, G.; Fercu, D.; Jacob, J. *Chem Phys* 1996, 204, 181.
- HyperChem Program Release 7.51 for Windows; Hypercube: Gainesville, FL, 2002.
- Doherty, D. *MOLSIM: Molecular Mechanics and Dynamics Simulation Software. User's Guide*; version 3.2; Chem21 Group: Lake Forest, IL, 1997.
- Dewar, M. J. S. E.; Zoebisch, G.; Healy, E. F.; Stewart, J. J. P. *AMI: J Am Chem Soc* 1985, 107, 3902.
- Weiner, S. J.; Kollman, P. A.; Nguyen, D. T.; Case, D. A. *J Comput Chem* 1986, 7, 230.
- Hopfinger, A. J. In *Conformational Properties of Macromolecules*; Academic Press: New York, 1973; p 71.
- Berendsen, H. J. C.; Postman, J. P. M.; van Gunsteren, W. F.; di Nola, A.; Haak, J. R. *J Chem Phys* 1984, 81, 3684.
- van Gunsteren, W. F.; Berendsen, H. J. C. *Angew Chem Int Ed Engl* 1990, 29, 992.
- Tokarski, J. S.; Hopfinger, A. J. *J Chem Inform Comput Sci* 1997, 37, 792.
- Rogers, D.; Hopfinger, A. J. *J Chem Inform Comput Sci* 1994, 34, 854.